

Development of Sponge Structure and Casting Conditions for Absorbable Magnesium Bone Implants

Stefan Julmi, Christian Klose, Ann-Kathrin Krüger, Peter Wriggers and Hans Jürgen Maier

Abstract In the case of bone defects, there are two different methods to close such defects. One option is to use bone autografts, but therefore the bone graft has to be cut off from the same person's hip. In this case the patient has to undergo an additional surgery, which bears complications, like causing inflammations. Absorbable, open-pored implants minimize these risks. Synthetic bone implants are typically made of ceramics, bioglass or polymers. In this study, magnesium alloys were investigated as absorbable porous bone substitute materials in which the bone can grow into. The main advantages are the design flexibility to produce individual implants by investment casting and mechanical properties similar to the bone. In order to adapt the degradation behavior to the bone's ingrowth behavior, the implant material has to be alloyed and coated. Moreover, to meet the mechanical requirements, finite element simulations of the sponge structure were used during the design phase of the structures and compression tests were conducted for experimental validation.

Keywords Sponge structure · Absorbable magnesium · Bone implants

Introduction

Natural bone is reconstructed continuously to repair defects and prevent ageing of the bone. Therefore the bone cells, i.e. osteoclasts, remove the old bone before the osteoblasts can rebuild the structure [1]. If a bone defect exceeds a critical size, the body's own healing mechanisms cannot close this defect. In this case the defect has to be closed by surgery. A widely used technique is the use of allogenic or

S. Julmi (✉) · C. Klose · H.J. Maier
Leibniz Universität Hannover, Institut für Werkstoffkunde (Materials Science),
An der Universität 2, Garbsen, 30823, Germany
e-mail: julmi@iw.uni-hannover.de

A.-K. Krüger · P. Wriggers
Leibniz Universität Hannover, Institute of Continuum Mechanics, Appelstraße 11,
Hannover, 30167, Germany

autologous bone grafts. When using the body's own bone, the patient has to undergo a second surgery, which can cause inflammation and pain [2]. Allogenic bone grafts can lead to infections or transmission of diseases [3].

To avoid these problems, synthetic materials can be used in bone substitute implants. Traditional implant materials for this application can be categorized in ceramics, bioglass, polymers and metals. Ceramics and polymers can be synthetic materials like zirconia (ZrO_2) and polymethylmethacrylate (PMMA) or natural materials like calcium phosphates (CaP) and collagen [4, 5].

Absorbable polymers do not have the necessary strength and can cause foreign body reactions. In contrast, ceramics show good biocompatibility and high strength, but the Young's modulus is higher than that of the bone, which may result in stress shielding. Additionally, they have low ductility and, as a result, might fail quickly under shifting loads.

Magnesium (Mg) alloys, which will be investigated in this study, have an elastic modulus near that of the human bone and show higher ductility than ceramics as well as good biocompatibility and a sufficient yield strength [6].

To adapt the mechanical properties to the requirements, the material can be alloyed. The degradation behavior can be adapted by alloying as well as by coating the material. Previous studies demonstrated a reduced corrosion rate of the Mg alloy LAE442 in comparison with other Mg alloys [7]. Furthermore, an increase of ductility is observed by alloying with lithium [8]. Moreover, alloying Mg with Lanthanum results in strengthening and a good corrosion resistance [9, 10].

In a related study, implants were produced by infiltration casting [11], but with this method, a reproducible, defined pore structure could not be achieved. In contrast, with the use of an investment casting process individual parts with defined geometry and a high design flexibility can be produced. The basis of the present approach is the generative production process called rapid prototyping (RP). This technology is now used not only in biomedical engineering, but also in other industries like aerospace. As it is the case in patient-individual implants, RP is predestined for the production of complex parts with a small production quantity. Another advantage is the possibility to simulate the mechanical behavior of the actual implant geometry under stress and the mold filling during the casting process to adjust the pore structure. The aim of this study was to obtain a structure that can be casted and has the mechanical properties needed for the application as a bone substitute material.

Materials and Methods

Magnesium Alloys

The Mg alloys LAE442 (4 wt% Li, 4 wt% Al, 2 wt% rare earth mischmetal, balance Mg) and La2 (2 wt% La, balance Mg) were used. The alloy LAE442 was produced as proposed by Seitz et al. [12] and the La2 alloy was produced according to Weizbauer et al. [13].

Simulation-Assisted Design of the Sponge Structure

There are three requirements to the implants. They must have a pore size between 150–500 μm for optimized bone ingrowth [4], they should carry the patient's load during the ingrowth time of the bone and the desired geometry has to be castable depending on the alloy, i.e. the mold has to be filled completely by the melt. Three different implant geometries were designed. The implants will be tested in a future in vivo study with rabbits and therefore the cylindrical implants had a diameter of 4 mm and a height of 5 mm. Using the CAD models, the stress distribution was simulated with a compressive load of 60 N, as it is the case in the loaded rabbit tibia [14]. For the simulation the magnesium alloy LAE442 was used with a yield strength of 148 MPa, a compressive yield point of 150 MPa and a compressive strength of 420 MPa [12]. The simulation was implemented in Abaqus by using a network of tetrahedrons and the cylindrical shaped bodies were loaded along the z-axis.

Casting Simulation and Investment Casting

The first step of the investment casting process was the implant's design using the CAD tool SolidWorks. The CAD model was then cut into layers with a thickness of 0.0127 mm. The sliced shape was then produced by a fused deposition modelling (FDM) method using a T612 3D printer (Solidscape, Inc., Merrimack, USA), with which the wax gating system was created. This casting tree was embedded in a special mold material for magnesium investment casting. In this case, Gilcast AM (BK Giulini GmbH, Ludwigshafen, Germany) was used. The curing process was carried out according to the manufacturer's instruction [15].

After curing, the mold was kept at 300 °C. The casting process was performed in a laboratory induction furnace MC50 (Indutherm GmbH, Walzbachtal-Wössingen, Germany) using a ceramic crucible with graphite lining. At first the furnace went through a preheating process to evaporate liquids and then the alloy was placed in the crucible. Before casting, the chamber underwent two cycles of evacuation and flushing with argon inert gas (Ar). Afterwards, the Ar pressure was set to 1 bar in order to prevent oxidation. To cast the alloy, the furnace was heated up to 740 °C with 40% of the heating capacity. Once the melting temperature was reached, the whole casting chamber was tilted in order to let the melt flow into the mold. After the casting process, the chamber stayed in the tilted position and a pressure of 2 bar of argon gas was applied in the casting chamber to promote the mold filling.

After demolding, the form filling was analyzed using a $\mu\text{CT}80$ computer tomograph (SCANCO Medical AG, Brüttisellen, Switzerland) with a nominal spatial resolution of 10 μm , an exposure time of 600 ms, a tube voltage of 70 kVp and a tube current of 114 μA . In the present study, a structure with a pore size of 400 μm based on the geometry of the structure with 500 μm was employed.

Compressive Test

To investigate the mechanical behavior under load, the implants were tested according to the standard DIN 50134 using a Z10 testing machine (Zwick GmbH & Co. KG, Ulm, Germany). The load velocity was adjusted to 10^{-2} s^{-1} . The ratio of length to diameter deviates from the standard of 1.5–2. The ratio used was chosen according to necessary size for the rabbits (length: 5 mm, diameter: 4 mm).

Results

Maximum Pore Size: 500 μm

The samples tested in this study are shown in Fig. 1. The models in Fig. 1 A and B are having a similar web thickness, while the vertical elements in model A are continuous along the z-axis and in model B the vertical elements are shifted. In model C the pores are more spherical with a narrow size distribution. Here, the struts are connected at right angles.

Mold Filling of the Structures in Fig. 1 with the Alloy LAE442

Figure 2 shows casted samples representative for the three different geometries. The two structures A and B with similar web thicknesses are completely filled with no cast defects or unfilled struts. By contrast, the molds of the samples in Fig. 1c were not all completely filled in the casting process and large parts of the samples show casting defects. In Fig. 2 the difference between the good and the defective samples can be seen clearly. Typical casting defects were not completely filled samples, broken bars or filled pores.

Mechanical Simulations

Due to the bad mold filling of the shape in Fig. 1c, only the mechanical simulations of the ones in Fig. 1a, b are compared in Fig. 3. If the shape has continuous elements in z-direction, the effective stress on the struts is lower. This allows for a better stress transmission along the z-axis. But this is only the case for a z-directed force.

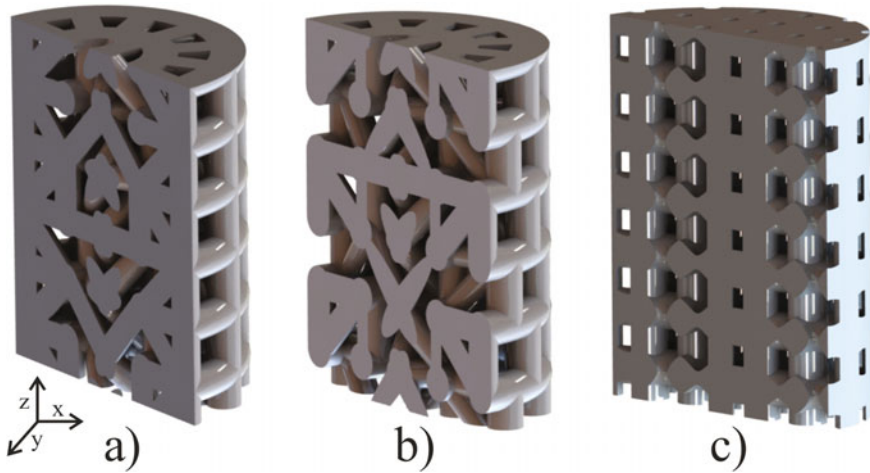
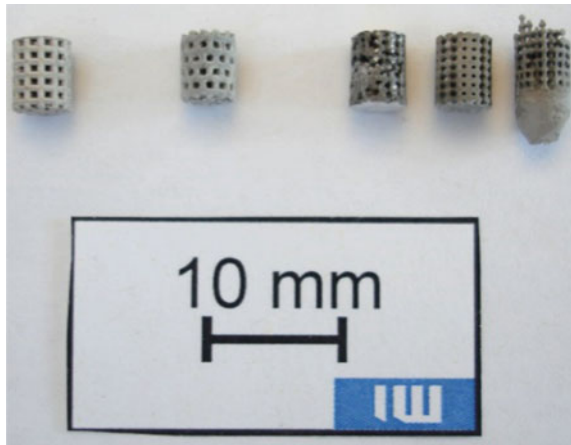


Fig. 1 Cross section of three different shapes designed with CAD

Fig. 2 Casted shapes of the previously mentioned structures. A is the on the *left*, followed by B and the three structures on the *right* are implants of the structure C



Due to the complete mold filling and the better behavior under stress, the shape with the continuous elements was slightly changed as it is shown in Fig. 4. In this final structure the struts have a thickness of 0.4 and 0.5 mm with a theoretical porosity of 41.35%. In Fig. 4 the CAD model is compared with the corresponding cast sample, recorded by μ CT. The overall structure of the cast shape corresponds with the designed shape for both alloys. All of the struts are filled, however the thickness varies and the surface is not as flat as in the CAD constructed file.

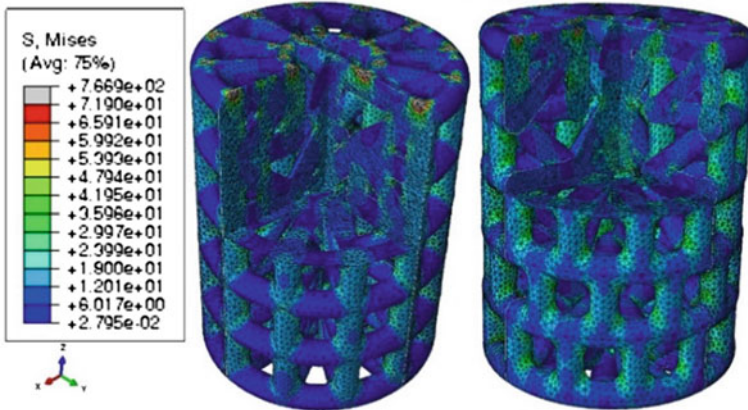


Fig. 3 Stress distribution in MPa of the structures a and b in Fig. 1 under the load of 60 N

Maximum Pore Size: 400 μm

Figure 5 shows a second shape, which was constructed on the basis of the previous experiments. The difference is that this structure has smaller elements and pores. In the model all the struts are having a thickness of 0.4 mm and the porosity is slightly lower (37.7%). As a result, the effective horizontal cross section area is larger. In the middle of the sample are irregularities. Here, it seems as if there are lots of small struts, but these are artefacts of the volume calculation by the CT. For this calculation the brightness range of the magnesium in the scans has to be set. But in this case there was still some gypsum in the middle of the shape and there is no hard transition in the brightness from the gypsum to the pores. As a result the gypsum couldn't be excluded completely for the calculation and also the solving process has to be further adjusted.

Mold Filling

As expected, the casting of finer structures is more challenging because the pores, which are filled with gypsum during the casting process, are smaller and therefore the gypsum is less stable. Additionally, the elements are smaller and therefore the melt solidifies earlier, which results in a not completely filled mold. Figure 5 shows that the structure can be filled completely, but the gating system has to be adapted in order to make the melt flow into the cavities with a smaller pressure thus preventing damage of the mold. Compared with the designed shape, the cast structure has the same derivations as in case of the structure with bigger pores. All the elements are filled, but there is a rougher surface.

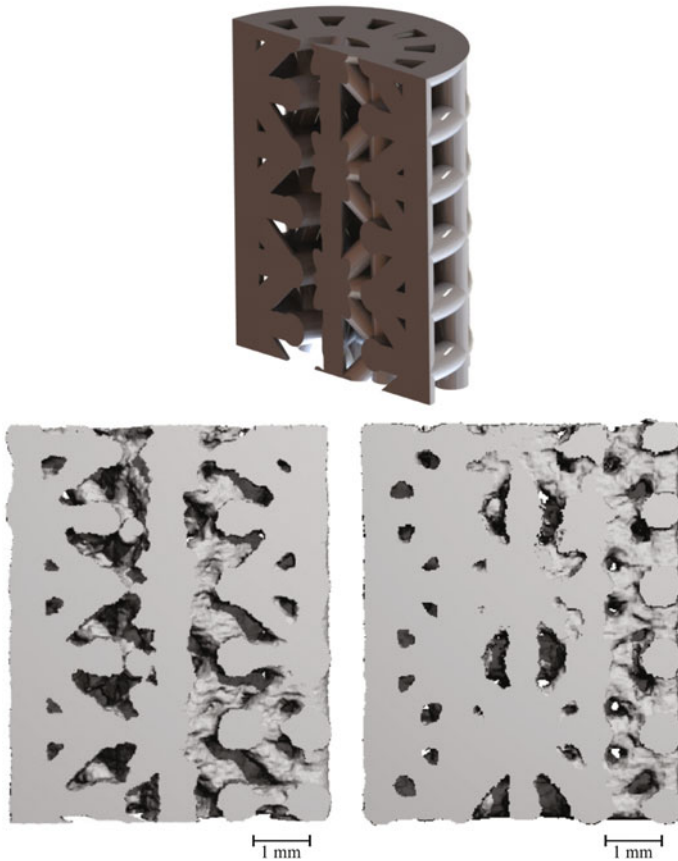


Fig. 4 CAD file and casted foam of the final shape for the implants with LAE442 on the *left* and La2 on the *right*

Mechanical Simulation

The stress distributions of the structures with maximum pore sizes of $500\ \mu\text{m}$ is in the range of 1.13–1.61 MPa. At the hubs the stress is locally higher and reaches up to 21.5 MPa. In the structure with a maximum pore size of $400\ \mu\text{m}$, the stress on the vertical elements between the horizontal elements with 5.4–10.8 MPa is significantly smaller. Only where the vertical elements cross the horizontal ones, the stress is in the range of 10.8–16.1 MPa. The lower stress is due to the larger effective cross section area (Fig. 6).

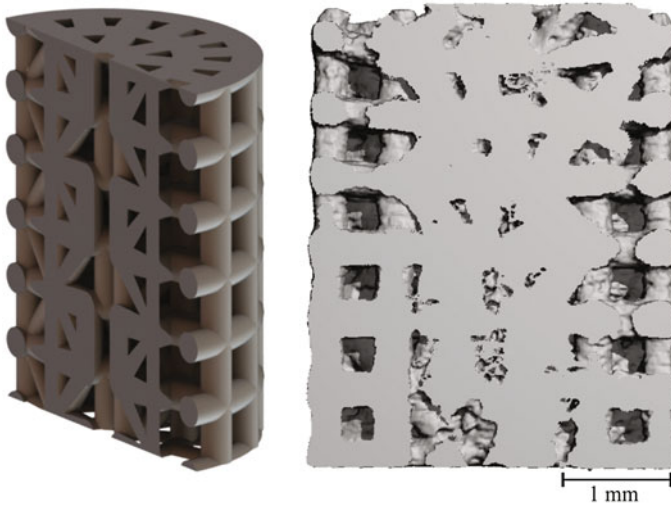


Fig. 5 CAD file and cast sample of the final shape with maximum pore size of 400 μm

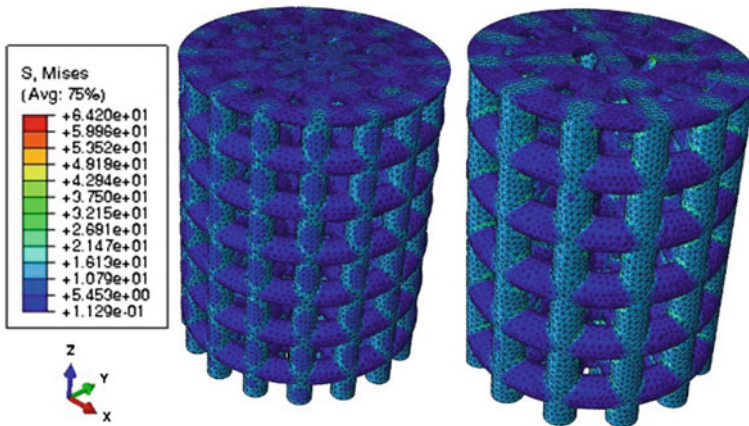


Fig. 6 Stress distribution of the structures in Figs. 3a and 5 under the load of 60 N in MPa

Compressive Tests

As shown in the force-strain-curves in Fig. 7 and the corresponding values in Table 1, with 341 N and 383 N, respectively, the compression yield point F_{dF} in both structures is well above the expected load of 60 N in the rabbit tibia, in which the implants should be inserted. After the elastic limit there is a long region of plastic deformation until the structure collapses. Depending on the structure, the implants have compressive strength of 1608 or 1921 N, with a corresponding deformation of 21.4 or 33.2%.

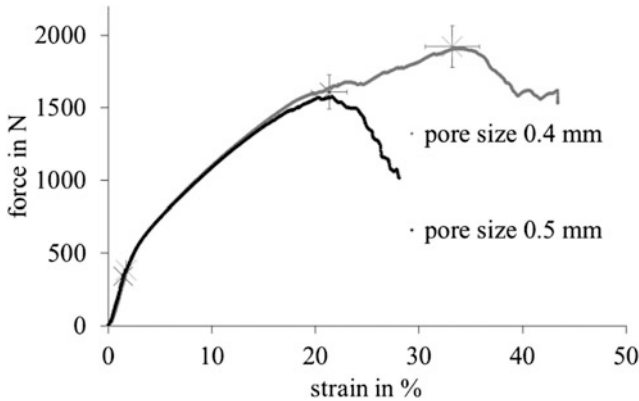


Fig. 7 Exemplary force-strain-diagram of one sample with larger pores (max. 0.5 mm) and one with smaller pores (max. 0.4 mm)

Table 1 Results of the compression test

Maximum pore size in mm	Compressive strength F_{\max} in N	Strain at F_{\max} in %	Compression yield point F_{dF} in N	Strain at F_{dF} in %
0.5	1608	21.4	341	1.45
0.4	1921	33.2	383	1.72

Discussion

The mold filling experiment has shown that the structure with the homogenous element thickness was filled completely, while several casting defects appeared in the other structures. The problem here is that the thickness of the elements is significantly smaller than 0.4–0.5 mm in some areas. Here, the melt can solidify faster, hence the elements can be blocked. In Fig. 2 an implant is shown in which some pores are filled. This suggests that the melt has broken some of the gypsum struts during the casting.

The structures with a complete mold filling and without defects are simulated for their stress distribution under a load of 60 N. This investigation has shown, that the effective stress is smaller, if the elements in z-direction (direction of the force in the experiments) are not tilted after every horizontal strut. If the struts are shifted, the stress lines are accumulated at the hubs, which causes higher stress peaks. Compared with the results of Seitz et al. [12], the simulated stress is lower than the experimentally determined yield point of 150 MPa. However, in the present study, the shapes were produced by investment casting whereas Seitz et al. used extruded materials. The production method has a large influence on the microstructure and accordingly the mechanical properties.

Based on the compression tests, the assumption made after the simulation, that the structures made of LAE442 are stable enough can be confirmed. The magnesium sponges in Figs. 4 and 5 have enough strength for the application as an implant in a rabbit tibia. Here the yield point is in both cases much larger than the required 60 N.

If the magnesium alloys LANd442, Nd2, ANd42 and LNd42 corrode, there is a significant volume loss and a loss in the three-point-bending strength [16]. It can be expected, that other mechanical properties are decreasing as well, because the corrosion leads to more defects and less material. The load will therefore be carried by a smaller cross-section, which results in a higher stress. Therefore, it is beneficial, that there is a buffer in the compression yield point.

Still there are other aspects, which have an influence on the corrosion, like saturation effects of the corrosion products [17].

Finally the bone ingrowth behavior, which depends on the pore size, is very important and degradation of the implant should be tailored accordingly. Therefore additional *in vivo* experiments are needed to find out which structure is stable long enough such that the bone can stabilize the defect.

The investigation of the casted structures with the CT showed that the whole structure could be casted close to the constructed shape. There is also no big difference between the two casted alloys. The LAE442 as well as the La2 alloy could fill the structure shown in Fig. 4. Furthermore the alloy LAE442 can fill the structure with the smaller pores and struts. The only differences are the rough surface and the different sizes in the struts. This is due to different process related reasons. The parts were first shaped layer by layer by FDM. This always results in a rougher surface in the z-direction, which cannot be compensated by surface treatments. Furthermore, the gypsum causes a rough surface depending on the size of the particles. The sponge-like structure however, has no serious defects or missing elements and can therefore be produced by investment casting.

Conclusion

In this study, a manufacturing process to produce sponge-like structures by investment casting was investigated and different implant geometries and alloys were simulated and casted. It has been demonstrated that the constructed shapes could be casted successfully by investment casting. Additionally, the implants appear to have a sufficient compressive strength and a pore structure that is necessary for an optimized bone ingrowth behavior.

Acknowledgements This research is sponsored by the German Research Foundation (DFG) within the project “Interfacial effects and ingrowing behavior of magnesium-based foams as bioresorbable bone substitute material” (grant no. MA 1175/52-1).

References

1. S.C. Manolagas, Birth and death of bone cells: basic regulatory mechanisms and implications for the pathogenesis and treatment of osteoporosis. *Endocr.Soc.* **21**(2), 115–137 (2000)
2. P.C. Missiuna et al., Anatomically safe and minimally invasive transcristal technique for procurement of autogenous cancellous bone graft from the mid-iliac crest. *Can. J. Surg.* **54**(5), 327–332 (2011)
3. A.J. Salgado, O.P. Coutinho, R.L. Reis, Bone tissue engineering: state of the art and future trends. *Macromol. Biosci.* **4**, 743–765 (2004)
4. Bone regeneration and repair, *Biology and Clinical Applications* (Humana Press Inc, Totowa, NJ, 2005)
5. T.V. Thamaraiselvi, S. Rajeswari, Biological evaluation of bioceramic materials: a review. *Trends Biomater. Artif. Organs* **18**(1), 9–17 (2004)
6. X. Gu, Y. Zheng, A review on magnesium alloys as biodegradable materials. *Frontiers Mater. Sci. China* **4**(2), 111–115 (2010)
7. F. Witte et al., In vivo corrosion of four magnesium alloys and the associated bone response. *Biomaterials* **26**, 3557–3563 (2005)
8. H. Haferkamp et al., Development, processing and applications range of magnesium lithium alloys. *Mater. Sci. Forum* **350–351**, 31–42 (2000)
9. T.L. Chia et al., The effect of alloy composition on the microstructure and tensile properties of binary Mg-rare earth alloys. *Intermetallics* **17**, 481–490 (2009)
10. N. Birbilis et al., On the corrosion of binary magnesium-rare earth alloys. *Corros. Sci.* **51**, 683–689 (2009)
11. F. Bach et al., Magnesium sponges as a bioabsorbable material: attributes and challenges. *Int. J. Mater. Res.* **98**, 609–612 (2007)
12. J. Seitz et al., The effect of different sterilization methods on the mechanical strength of magnesium based implant materials. *Adv. Eng. Mater.* **13**, 1146–1151 (2011)
13. A. Weizbauer et al., Novel magnesium alloy Mg–2La caused no cytotoxic effects on cells in physiological conditions. *Mater. Sci. Eng. C* **41**, 267–273 (2014)
14. J. Reifenrath et al., Axial forces and bending moments in the loaded rabbit tibia in vivo. *Acta Vet. Scand.* **54**(21), 1–7 (2012)
15. Giullini, http://bk-giullini-pcg.com/Deutsch/Gips/Giesserei_Modellbau/Giesserei.htm. Accessed 27 June 2016
16. J. Seitz et al., Comparison of the corrosion behavior of coated and uncoated magnesium alloys in an in vitro corrosion environment. *Adv. Biomater.* **13**, B1–B11 (2011)
17. X. Gu et al., In vitro corrosion and biocompatibility of binary magnesium alloys. *Biomaterials* **30**, 484–498 (2009)